Supporting Information

Near-Infrared Emitting Squaraine Dyes with High 2PA Cross Sections for Multiphoton Fluorescence Imaging

Hyo-Yang Ahn,[a] *Sheng Yao,*[a] *Xuhua Wang,*[a] *and Kevin D. Belfield*[*a,b]

[a] Department of Chemistry and [b]CREOL, The College of Optics and Photonics,

University of Central Florida, P.O. Box 162366, Orlando, FL 32816-2366, USA

1 ^{1}H NMR and ^{13}C NMR spectra

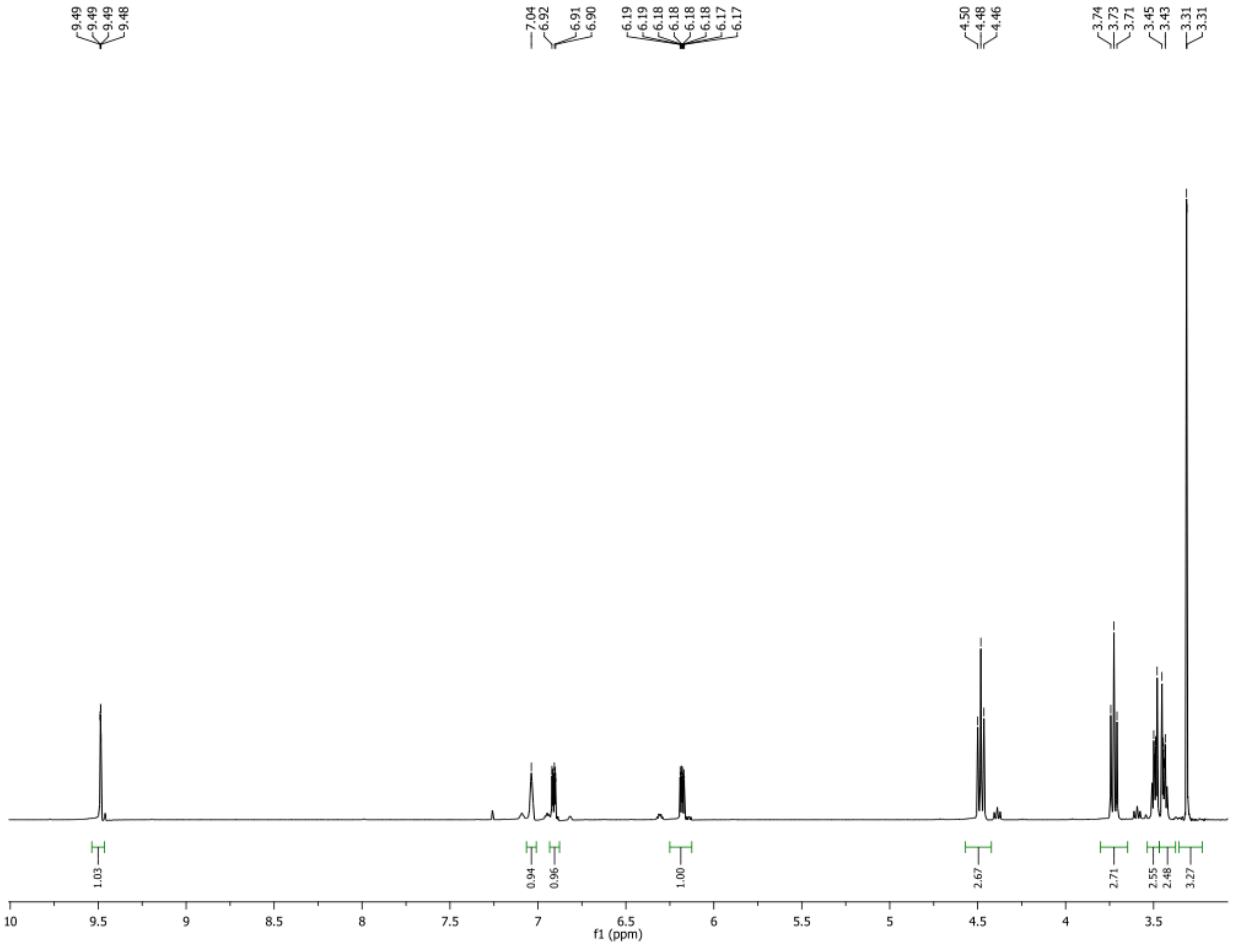

Figure S1. ^{1}H NMR spectrum of compound **3**.

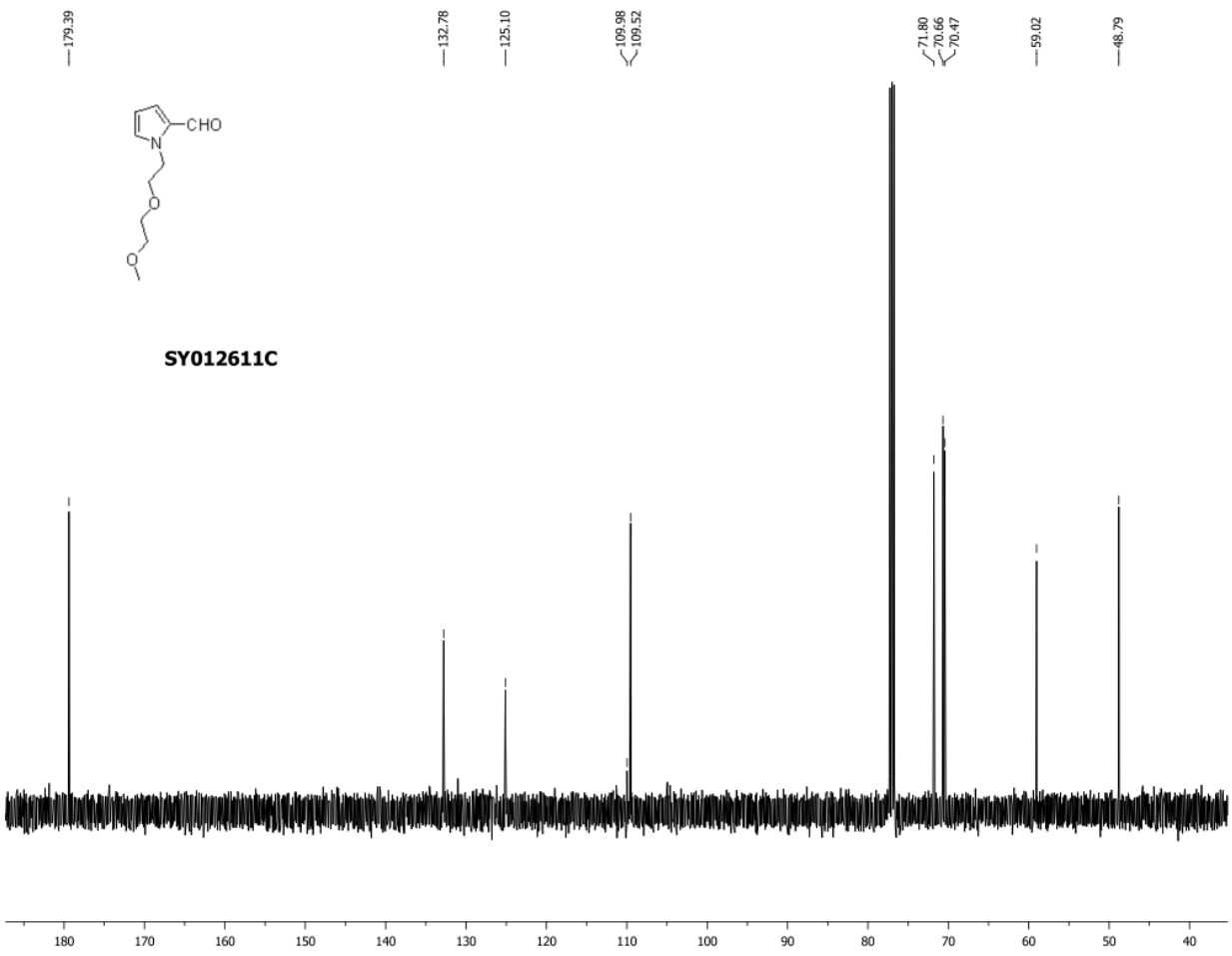

Figure S2. ^{13}C NMR spectrum of compound **3**.

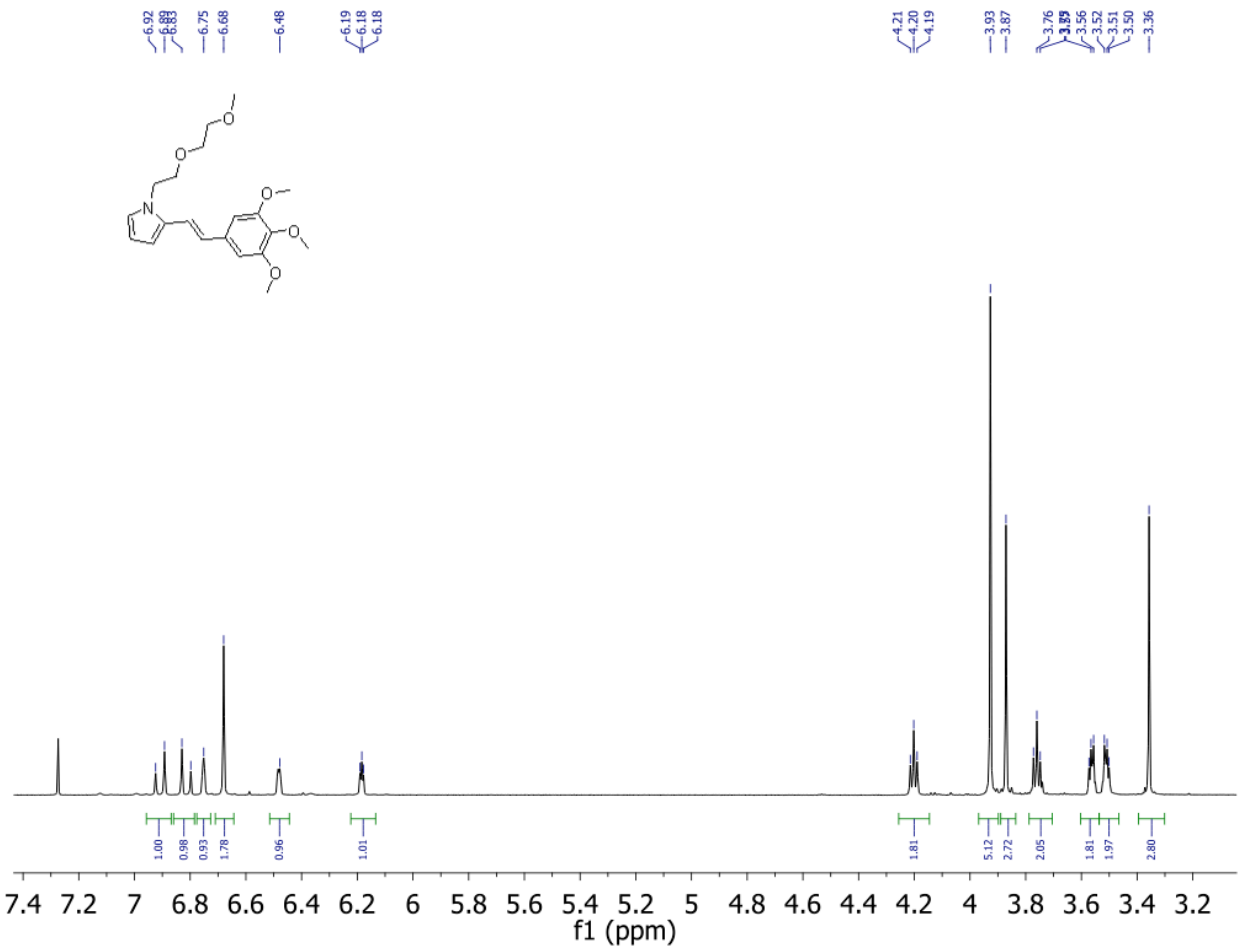

Figure S3. ^{1}H NMR spectrum of compound **4**.

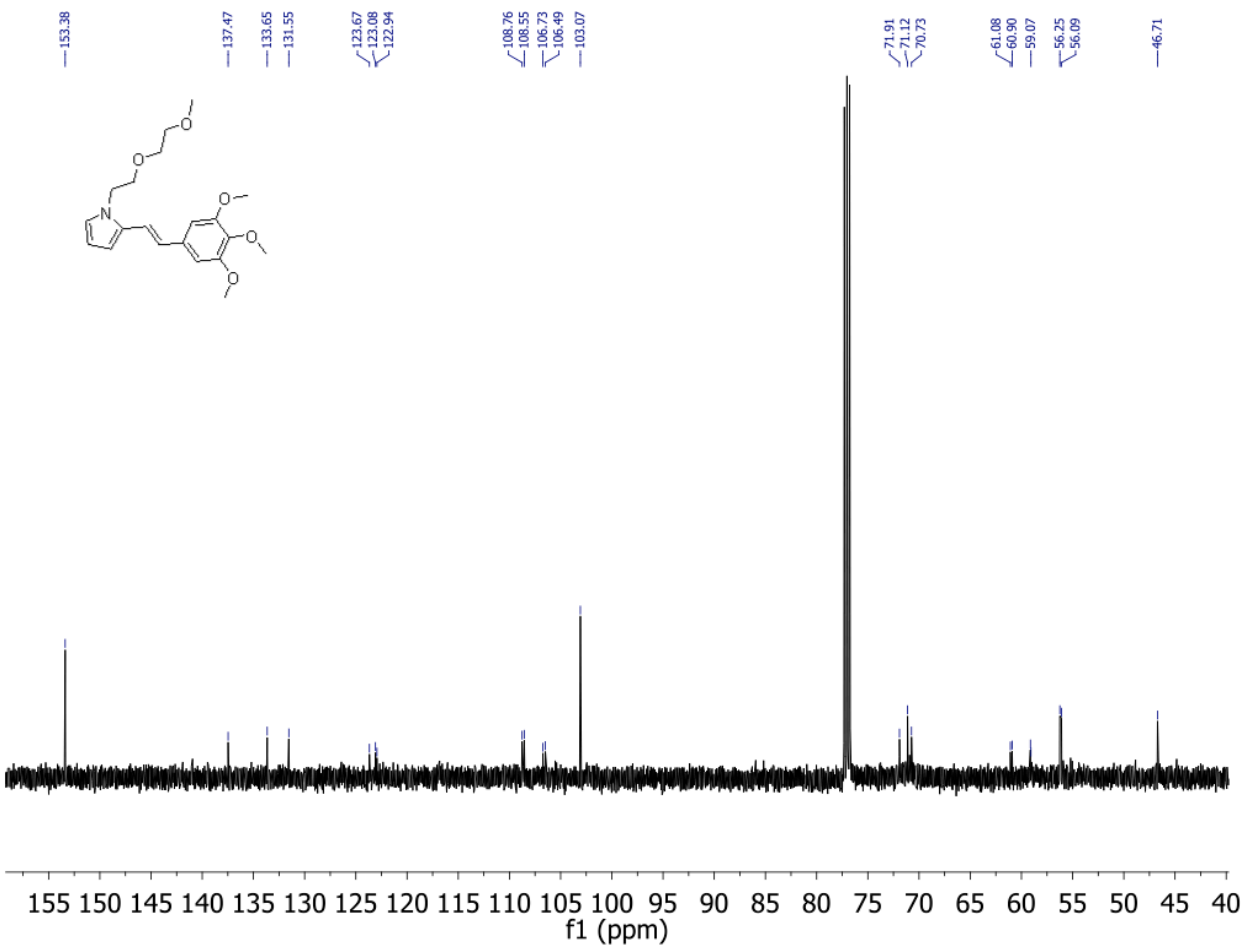

Figure S4. ^{13}C NMR spectrum of compound **4**.

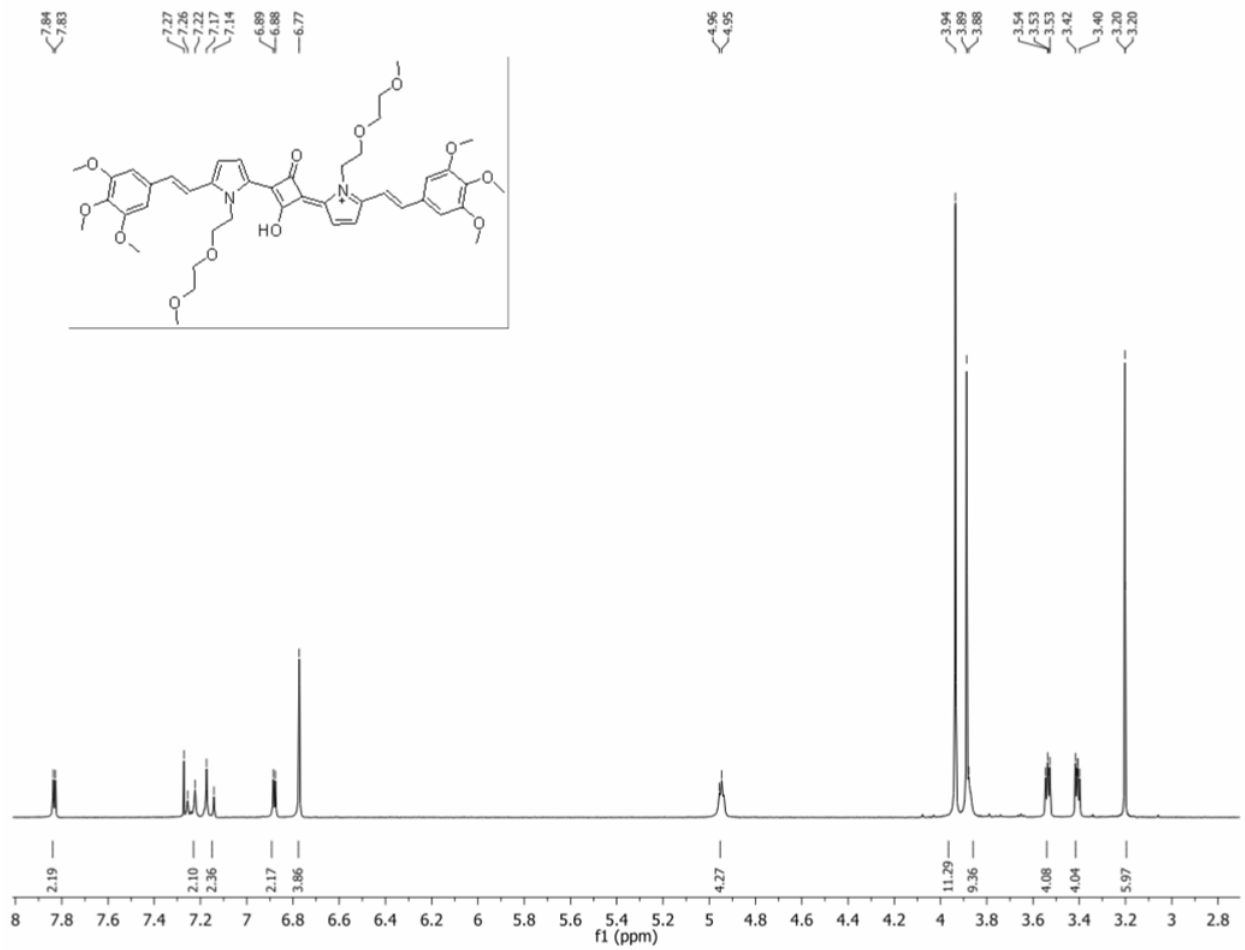

Figure S5. ^{1}H NMR spectrum of SQ **1**.

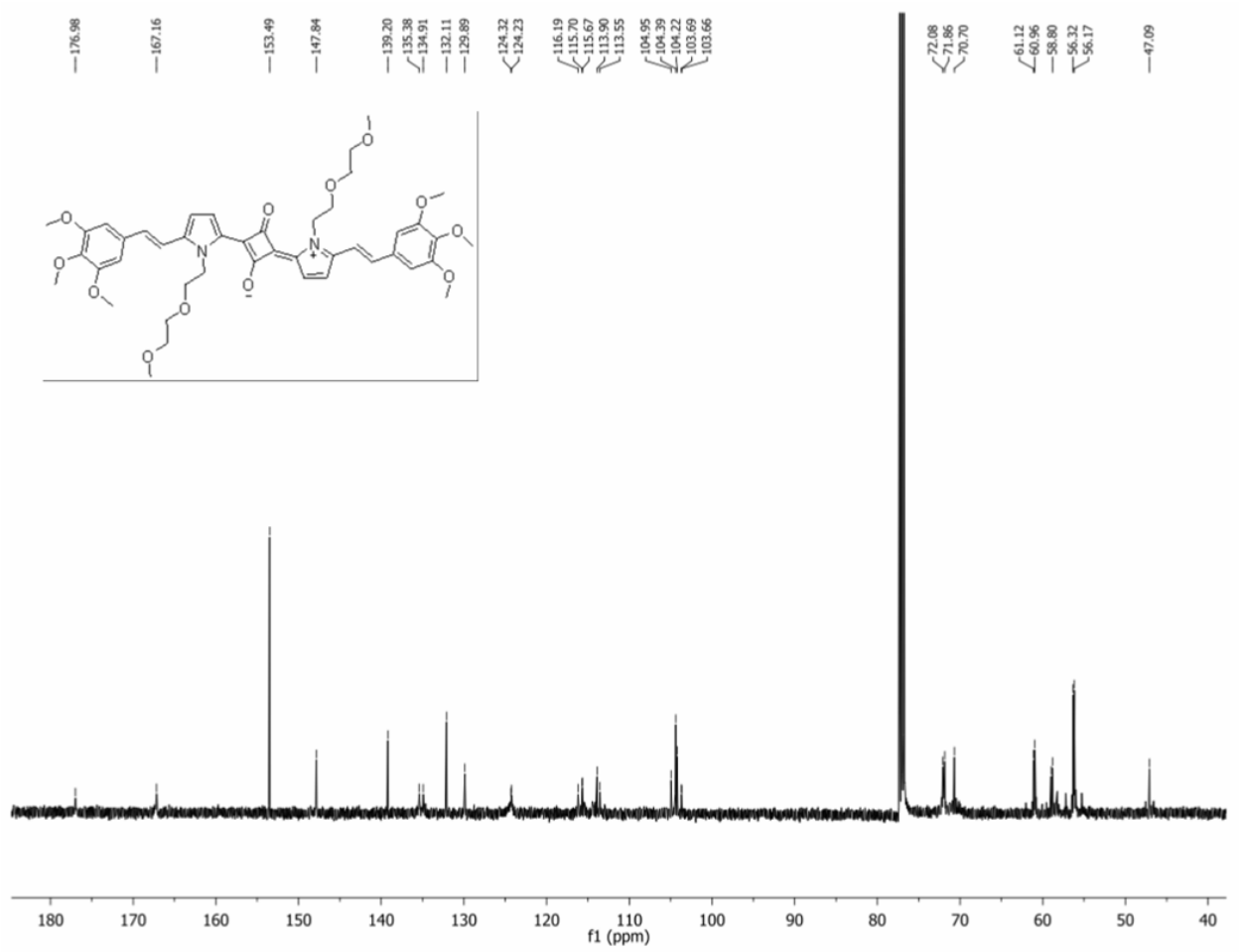

Figure S6. ^{13}C NMR spectrum of SQ **1**.

2 Linear spectroscopic measurements

Absorption spectra were measured by Agilent 8453 UV-vis spectrophotometer. Fluorescence emission and excitation spectra were measured using a PTI Quantamaster Spectrofluorimeter with a Hamamatsu R928 photomultiplier tube (PMT) in acetonitrile (ACN), 1, 2-dichloromethane (DCM), DMSO, MeOH, and THF for SQ**1** (Figure S7) and SQ **2** (Figure S8).

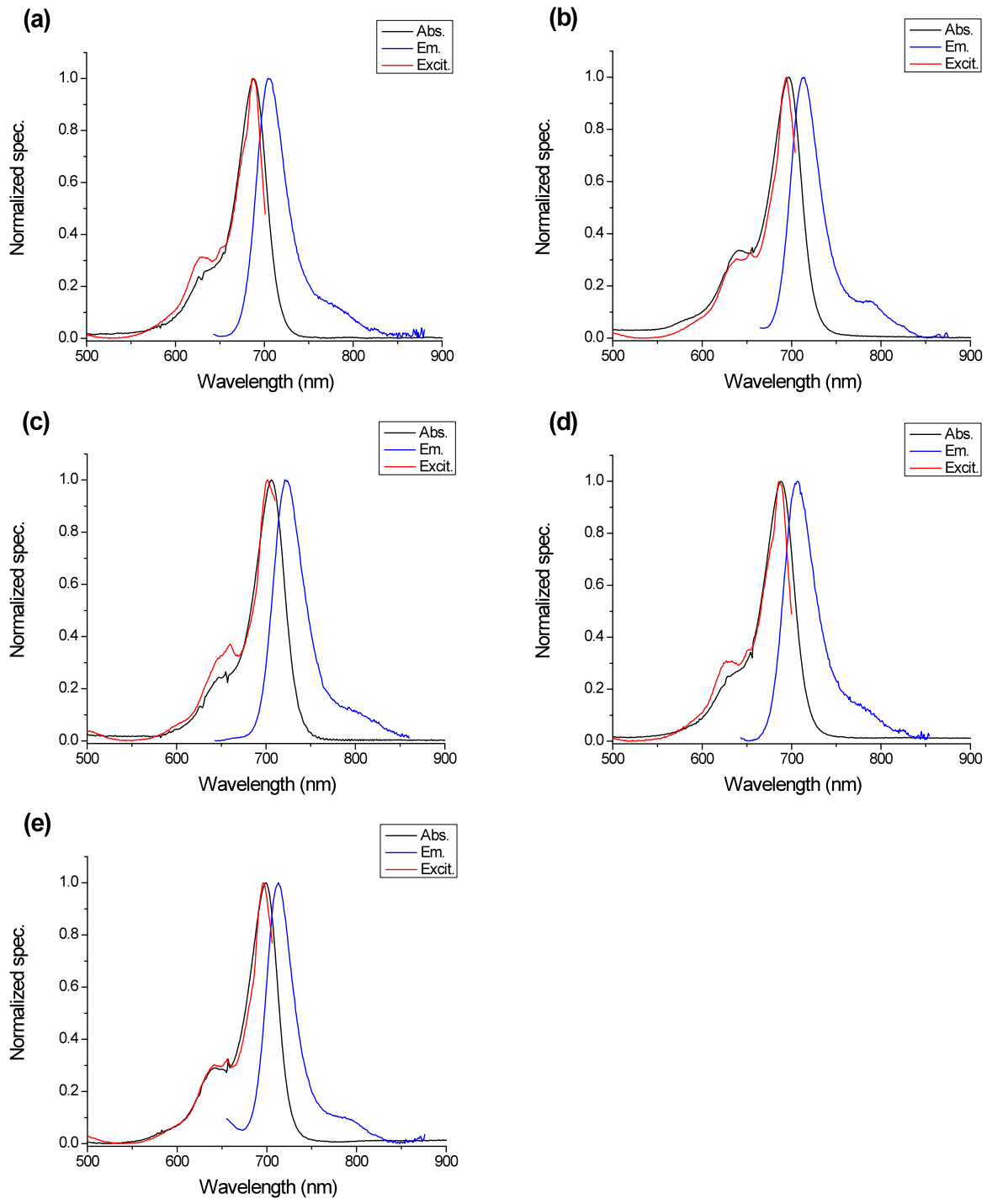

Figure S7. Absorption, fluorescence emission, and excitation spectra of SQ **1** in (a) ACN, (b) DCM, (c) DMSO, (d) MeOH, and (e) THF.

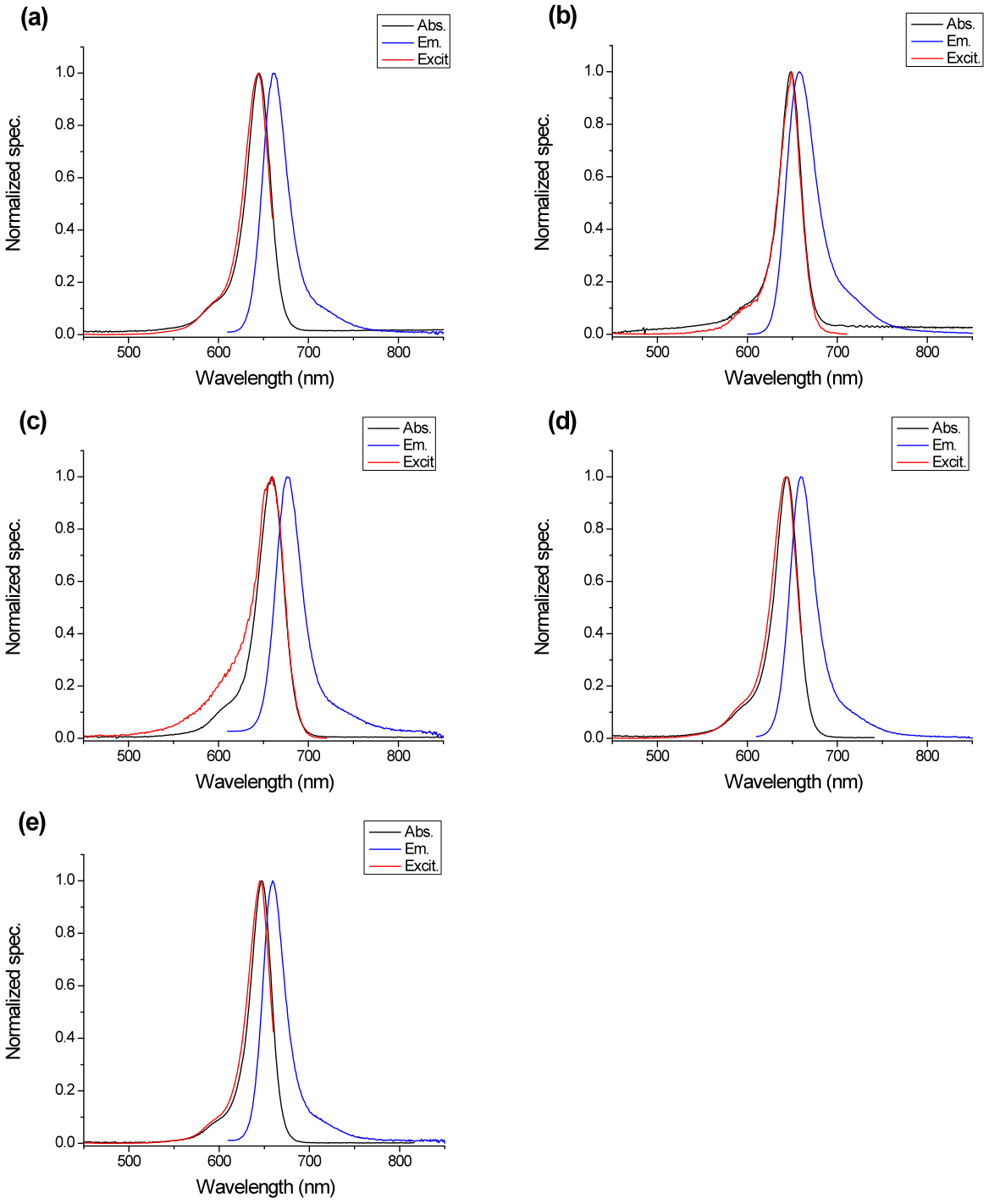

Figure S8. Absorption, fluorescence emission, and excitation spectra of SQ **2** in (a) ACN, (b) DCM, (c) DMSO, (d) MeOH, and (e) THF.

3 Photostability measurements

The photochemical stability (photodecomposition quantum yield) evaluations of squaraines **1** and **2** along with **Cy5** in DMSO were conducted by irradiating with the output of a 650 nm diode laser[1] (75 mW) of an Ar-degased solution in a 10 mm path length quartz cuvette. Kinetic changes in the absorption spectra were monitored with an Agilent 8453 UV-vis spectrophotometer (Figure S9).

Photodecomposition quantum yields, η, were calculated as follows,[1]

$$\eta = \frac{(A_1 - A_0)N_A}{\varepsilon I\left(1 - 10^{\frac{A_1+A_0}{2}}\right)(t_1 - t_0)}$$

where η is the photochemical decomposition quantum yield, A_1 is absorbance maxim at t_1, A_0 is absorbance max at t_0, N_A is Avogadro's number, ε is molar absorbance in $M^{-1}\cdot cm^{-1}$, $(t_1\text{-}t_0)$ is time exposed (s), and I is the intensity of laser in photon$\cdot cm^{-2}\cdot s^{-1}$.

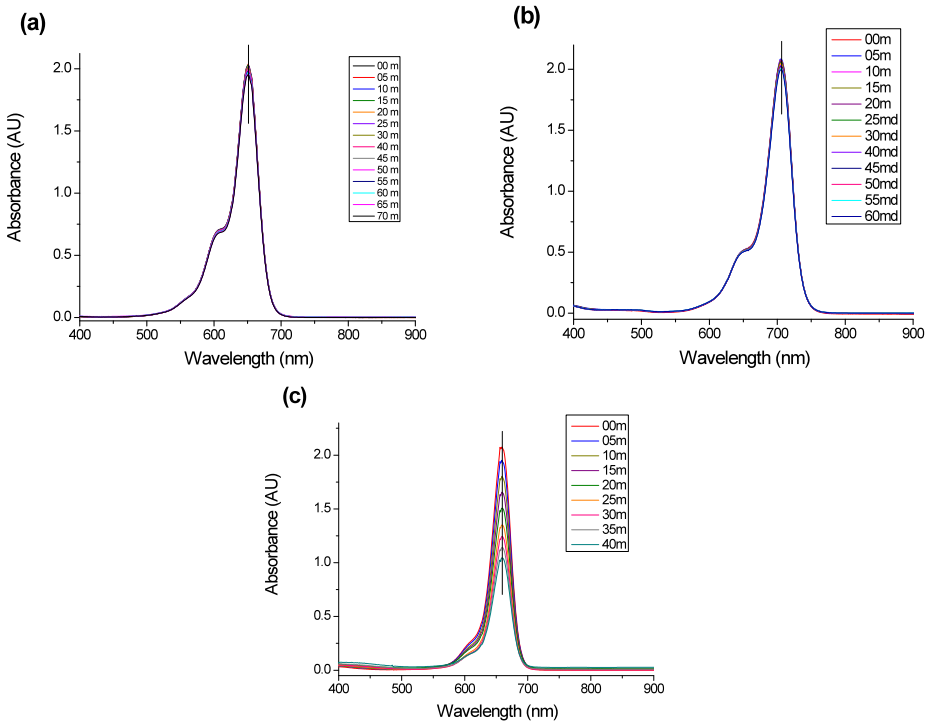

Figure S9. Time-dependent absorption spectra of corresponding dyes with irradiation at 650 nm for DMSO solutions of (a) **Cy5**, (b) SQ **1**, and (c) SQ **2**.

4 Thermostability of squaraines 1 and 2

Thermostability study was conducted by thermogravimetric analysis (TGA, Q 5000 TA Instruments) and differential scanning calorimetry (DSC, Q1000 TA Instruments), as shown in Figure S10.

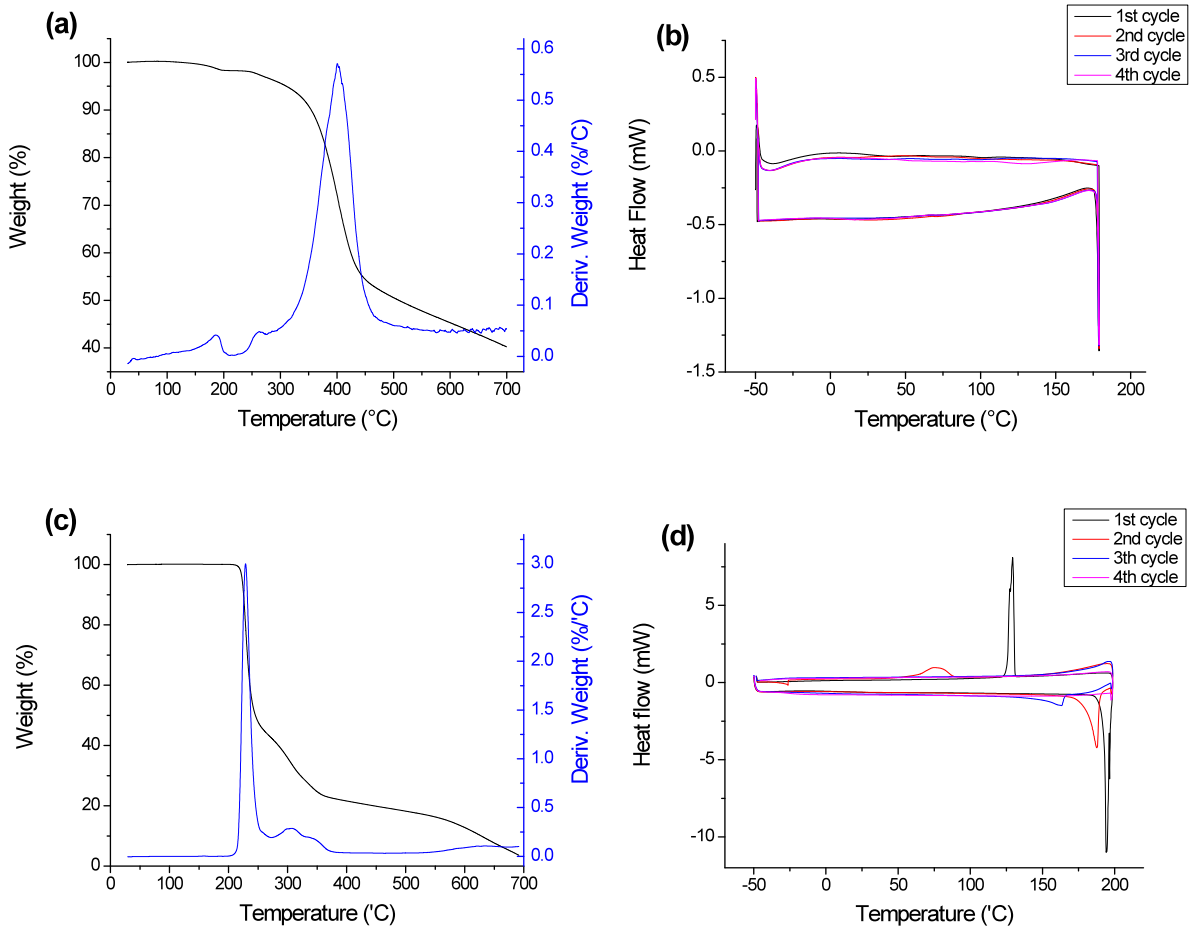

Figure S10. a) TGA and (b) DSC analyses of SQ **1**, and (c) TGA and (d) DSC analyses of SQ **2**.

5 Linear and nonlinear optical properties of Cy5

The absorption and fluorescence emission spectra of **Cy5** (Figure S11) were measured in DMSO with an Agilent 8453 UV-vis spectrophotometer and PTI Quantamaster Spectrofluorimeter, respectively. 2PA measurements (Figure S11) were performed using a tunable fs Ti:sapphire laser system (Coherent MIRA 900, pulse duration ~200 fs/pulse (FWHM), repetition rate 76 MHz) coupled with a PTI Spectrofluorimeter system via a fluorescence method. The two-photon absorption cross section was calculated as follows;

$$\delta_{2PA-s} = \delta_{2PA-r} \frac{\Phi_r}{\Phi_s} \frac{C_r}{C_s} \frac{< F >_s}{< F >_r} \frac{n_s}{n_r} \frac{< P_r >^2}{< P_s >^2}$$

where subscripts *R* and *S* refer to the reference and sample, respectively, Φ is fluorescence quantum yield, *C* is the concentration, *F* is the integrated area, *n* is the refractive index of the solvent, and *P* is the incident power of the laser. The experimental fluorescence excitation and detection conditions were measured with negligible reabsorption.[2] The quadratic dependence of two-photon induced fluorescence intensity on the excitation power was verified for each excitation wavelength.

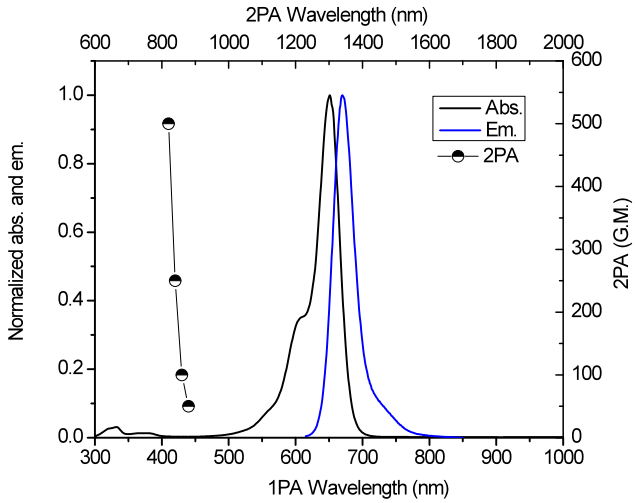

Figure S11. Linear and nonlinear optical characterization of **Cy5** (1 GM (Göppert Meyer) = 10^{-50} cm^4 s/photon^{-1}, uncertainty of the 2PA value = 15 %), absorption (black), emission (blue), and 2PA cross sections (black circles).

6 Linear and nonlinear properties of micelles

The open aperture Z-scan method[3] was performed to measure 2PA cross sections of micelle-encapsulated squaraines **1** and **2** along with **Cy5** (Figure S12), using a fs Ti:sapphire amplified system (Coherent, MIRA and Legend) with an optical parametric amplifier (model OPerA) providing laser pulses ~100 fs (FWHM) duration with 1 kHz repetition rate. The concentration of solution concentration was ca. 10^{-3} M in a 1 mm quartz cuvette at room temperature.

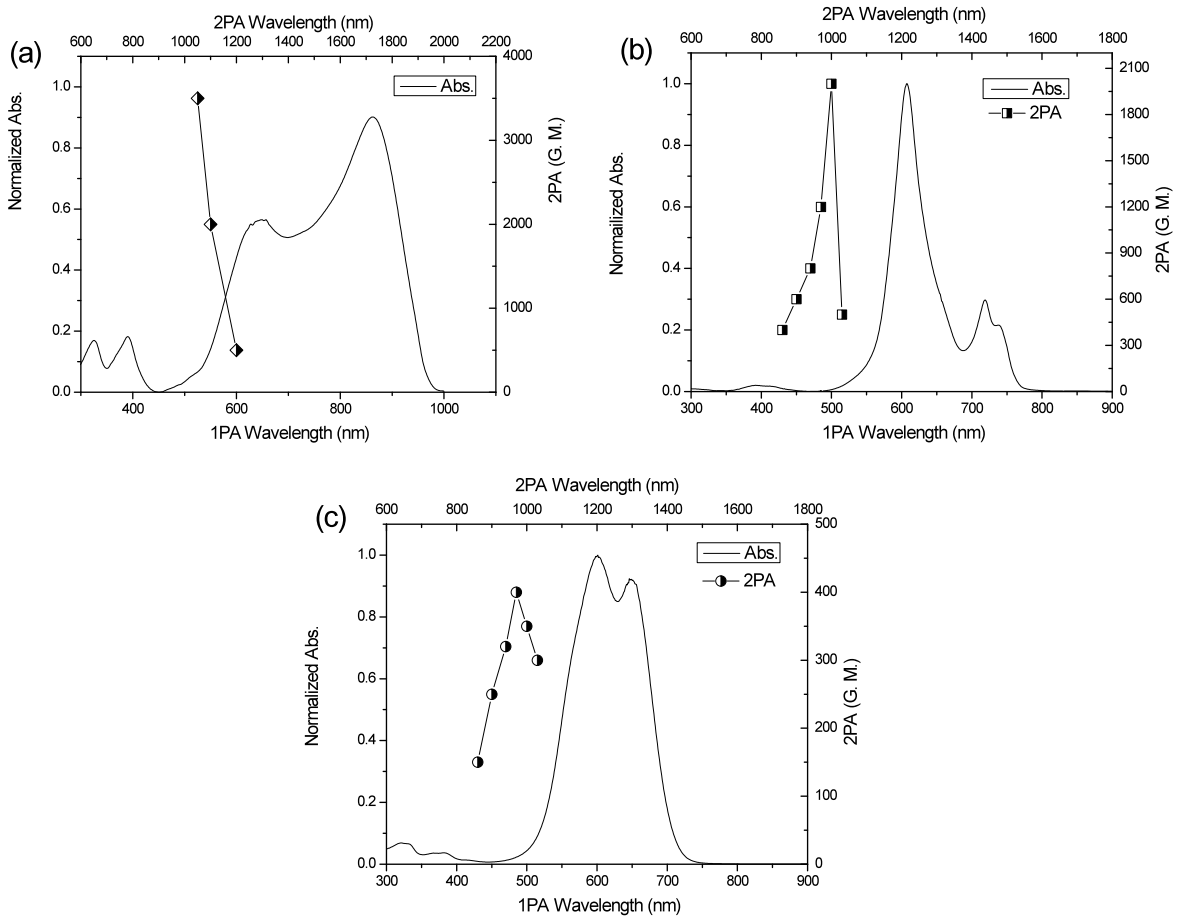

Figure S12. Linear and nonlinear optical characterization of micelle mixtures of (a) SQ **1**, (b) SQ **2**, and (c) **Cy5** (error ± 25%).

7 Cytotoxicity assays of squaraines 1 and 2 in HCT 116 and COS 7

HCT116 and COS 7 cells were prepared for cytotoxicity tests and incubated for 20 h with the SQ dye encapsulated in micelles, followed by further incubation additional for 4 h with CellTiter 96® Aqueous One Solution reagent (MTS assay) at 37 °C (Figure S13).

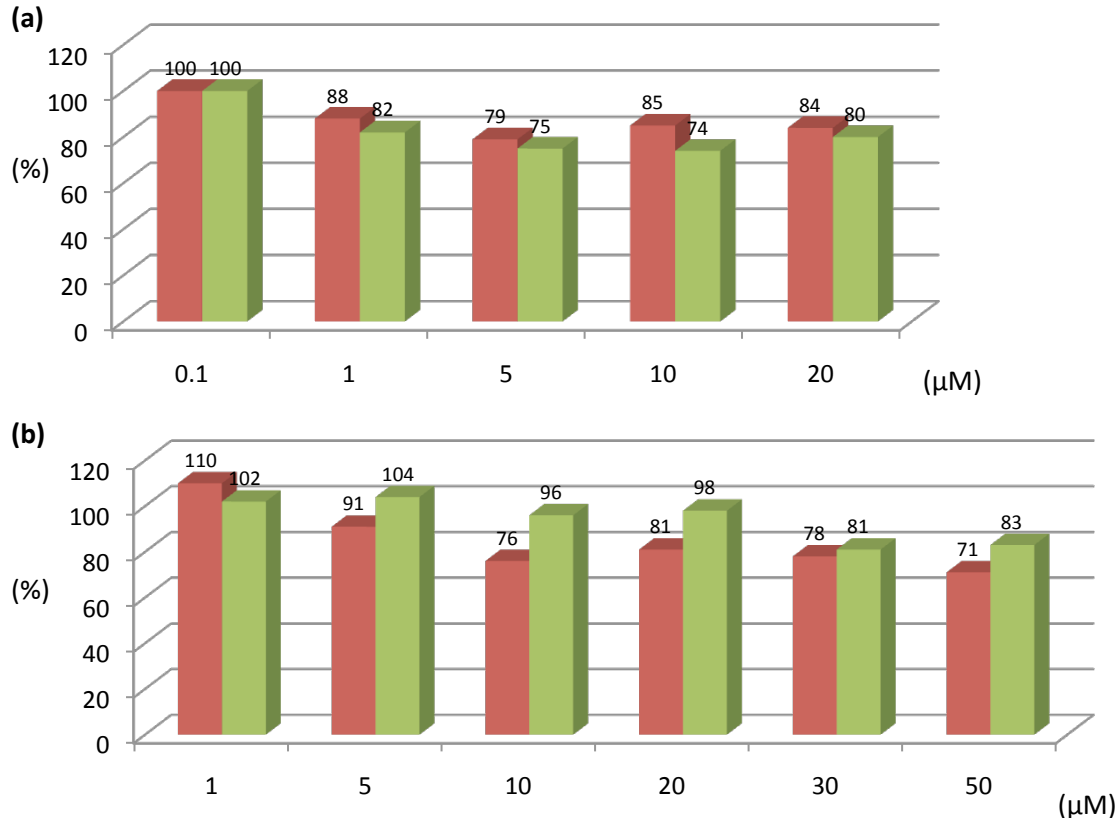

Figure S13. Cell viability of (a) SQ **1** and (d) SQ **2** in HCT 116 and COS 7 cells (error ±10 %).

8 1PFM images of squaraine 1 and 2 in HCT 116 and COS 7

A confocal microscope system (Olympus IX70/Fluoview 300) equipped with a QImaging cooled CCD (Model Retiga EXi) and mercury lamp 100 W was used for 1PFM imaging of HCT 116 cells with SQ **1** (Figure S14) and SQ **2** (Figure S15) and COS 7 cells with SQ **1** (Figure S16) and SQ **2** (Figure S17), followed by staining with a Hoechst nuclear stain, using a 60× microscopic objective (UPlanSApo 60×, NA = 1.35, Olympus).

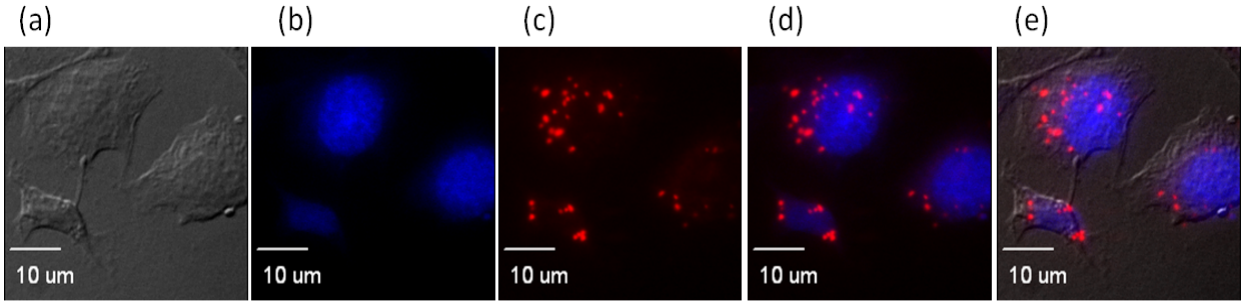

Figure S14. HCT 116 of 20 μM SQ **1** (a) DIC, (b) 1PA image with Fluo out (Ex 377/50, DM 409, Em 525/40), (c) 1PA image with Cy5 filter (Ex 630/50, DM 660, Em 690/40), (d) 1PA overlaid fluorescence image, (e) 1PA overlaid image (a) to (c) (scale bar = 10 μm). Emission from SQ **1** is in red while the emission from Hoechst is in red.

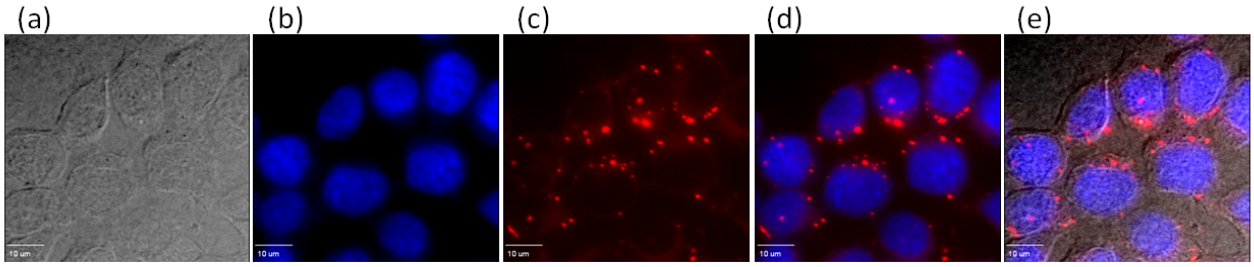

Figure S15. HCT 116 of 20 μM SQ **2** (a) DIC, (b) 1PA image with Fluo out (Ex 377/50, DM 409, Em 525/40), (c) 1PA image with Cy 5 filter (Ex 630/50, DM 660, Em 690/40), (d) 1PA overlaid fluorescence image, (e) 1PA overlaid image (a) to (c) (scale bar = 10 μm). Emission from SQ **2** is in red while the emission from Hoechst is in red.

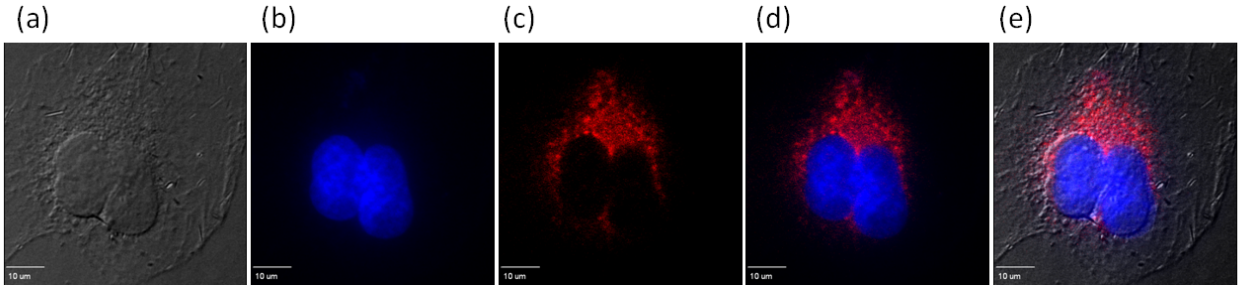

Figure S16. COS 7 of 20 μM SQ **1** (a) DIC, (b) 1PA image with Fluo out (Ex 377/50, DM 409, Em 525/40), (c) 1PA image with Cy 5 filter (Ex 630/50, DM 660, Em 690/40), (d) 1PA overlaid fluorescence image, (e) 1PA overlaid image (a) to (c) (scale bar = 10 μm). Emission from SQ **1** is in red while the emission from Hoechst is in red.

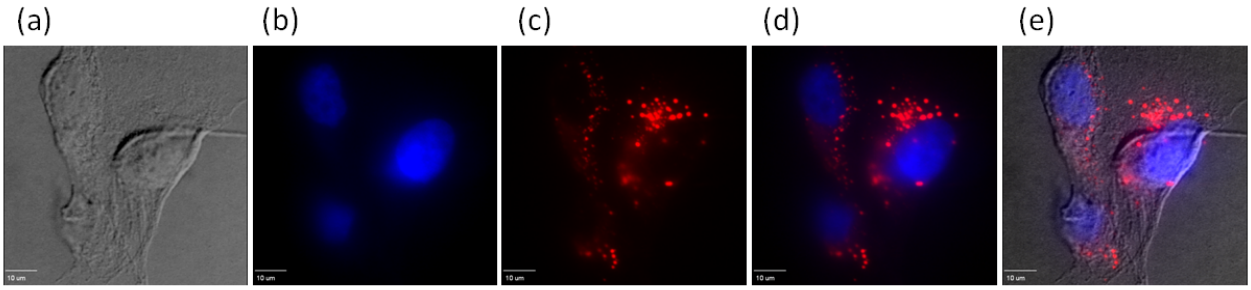

Figure S17 COS 7 of 20 μM SQ **2** (a) DIC, (b) 1PA image with Fluo out (Ex 377/50, DM 409, Em 525/40), (c) 1PA image with Cy 5 filter (Ex 630/50, DM 660, Em 690/40), (d) 1PA overlaid fluorescence image, (e) 1PA overlaid image (a) to (c) (scale bar = 10 μm). Emission from SQ **2** is in red while the emission from Hoechst is in red.

References

(1) Corredor, C. C.; Belfield, K. D.; Bondar, M. V.; Przhonska, O. V.; Yao, S. *J. Photochem. Photobiol., A* **2006**, *184*, 105-112.

(2) Belfield, K. D.; Bondar, M. V.; Hales, J. M.; Morales, A. R.; Przhonska, O. V.; Schafer, K. J. *J. Fluoresc.* **2005**, *15*, 3-11.

(3) Sheik-bahae, M.; Said, A. A.; Wei, T.-h.; Hagan, D. J.; Van Stryland, E. W. *IEEE J. Quantum Electron.* **1990**, *26*, 760-769.